An application of neural network for Structural Health Monitoring of an adaptive wing with an array of FBG sensors

Journal of Physics: Conference Series **305** (2011) 012066 doi:10.1088/1742-6596/305/1/012066

An application of neural network for Structural Health Monitoring of an adaptive wing with an array of FBG sensors

Magdalena Mieloszyk[1], Marek Krawczuk[2], Lukasz Skarbek[3] and Wieslaw Ostachowicz[3]

[1]IFFM PASci, Fiszera14, 80–952 Gdansk, Poland,

[2]IFFM PASci, Fiszera 14, 80–952 Gdansk and Technical University of Gdansk, Wlasna Strzecha 18a Street, 80–233, Gdansk, Poland,

[3]IFFM PASci, Fiszera14, 80–952 Gdansk, Poland,

[4]IFFM PASci, Fiszera14, 80–952 Gdansk and Gdynia Maritime University, Faculty of Navigation, Al. Jana Pawła II 3, 81–345, Gdynia, Poland,

E-mail: mmieloszyk@imp.gda.pl

Abstract This paper presents an application of neural networks to determinate the level of activation of shape memory alloy actuators of an adaptive wing. In this concept the shape of the wing can be controlled and altered thanks to the wing design and the use of integrated shape memory alloy actuators. The wing is assumed as assembled from a number of wing sections that relative positions can be controlled independently by thermal activation of shape memory actuators. The investigated wing is employed with an array of Fibre Bragg Grating sensors. The Fibre Bragg Grating sensors with combination of a neural network have been used to Structural Health Monitoring of the wing condition.
The FBG sensors are a great tool to control the condition of composite structures due to their immunity to electromagnetic fields as well as their small size and weight. They can be mounted onto the surface or embedded into the wing composite material without any significant influence on the wing strength.
The paper concentrates on analysis of the determination of the twisting moment produced by an activated shape memory alloy actuator. This has been analysed both numerically using the finite element method by a commercial code ABAQUS® and experimentally using Fibre Bragg Grating sensor measurements. The results of the analysis have been then used by a neural network to determine twisting moments produced by each shape memory alloy actuator.

1. Introduction

The high complexity and costs of aircraft structures combined with their high operational reliability and safety needs results in increasing interest in structural health monitoring (SHM) systems [7]. Fibre Bragg Grating (FBG) sensors are an interesting tool for SHM applications. The advantages of FBG sensors such as their small size, high multiplexing capabilities, corrosion resistance and good compatibility with the most advanced composite materials exploited in the aeronautics and aerospace fields [1] made them a good tool for measuring strain within structures as well as employing them for

monitoring the level of activation of shape memory alloy (SMA) actuators being a part of the adaptive wing under investigation.

Shape memory alloys (SMAs) are a class of smart materials that remember their original, low-temperature shape and they return to that shape after deformation by applying heat. SMAs components in the form of wires, strips, beams, etc. may be integrated within elements of structures in order to improve or control their static or dynamic performance. Taking into account the available range of various controllable properties of SMAs they can be effectively used in the active control of various static and dynamic characteristics of structural elements. For example, static deflection [4], [6], natural frequencies [5], [8], modes of vibration [2] and amplitudes of forced vibration [9] of the host structures can all potentially be changed, controlled or manipulated in a very precise manner by the use of embedded SMAs.

The authors have presented an application of neural network for SHM of an adaptive wing with an array of FBG sensors. In this concept the shape of the aircraft wing can be controlled and changed thanks to the wing design and the use of integrated SMA actuators. The prototype of the wing was constructed in IFFM PASci [3].

In the SMA actuators being a part of the adaptive wing a two-way shape memory effect was used. The FBG sensor configuration was able to measure changes in the longitudinal strain that were a result of activation of any of SMA actuator. This allows the authors to measure hysteresis visible during consecutive activation and deactivation processes for different configurations of activation of SMA actuators being a part of the wing.

This paper presents the application of neural networks to determinate the level of activation of SMA actuators of the adaptive wing. There is also presented an analysis of the determination of the twisting moment produced by activated SMA actuators. This has been analysed both numerically using the finite element method by a commercial code ABAQUS® and experimentally using FBG sensor measurements. The results of the analysis have been then used by a neural network to determine twisting moments produced by each SMA actuator.

2. An adaptive wing

The adaptive wing analysed in the paper consists of five sections: four of them being independent, while one section is fixed, providing necessary boundary conditions. The four independent sections were linked together at actuation points (denoted as A_1–A_4) on the common rotational axis (Figure 3). It was assumed that the actuation is a pure twist produced by four specially attached SMA wires. Based on the design the maximum level of actuation defined in terms of the actuation twisting moments for each SMA actuator was assumed as 0.2 Nm (counter-clockwise only). The assumed value based on the analytical calculations performed during designing process of the wing prototype. The total length of the wing was 1000 mm and its span was 250 mm. As a wing profile the Clark-Y aerofoil was chosen. The thickness of each profile is 10 mm, while the diameter of the common supporting rod is 25 mm. For the material for all wing sections and the supporting rod, aluminium alloy 2024- T3 was selected, while it was assumed that the outer wing skin is made out of 0.1 mm thick composite skin [3].

A finite element model of the adaptive wing is presented in Figure 1. As a modelling tool the finite element package ABAQUS® was used. For the finite element model of the adaptive wing 6398 elements were used in total, while the number of model degrees of freedom was 23 422. For modelling

the internal part of the wing three-dimensional finite elements were employed and the outer skin of the wing was modelled by shell finite elements.

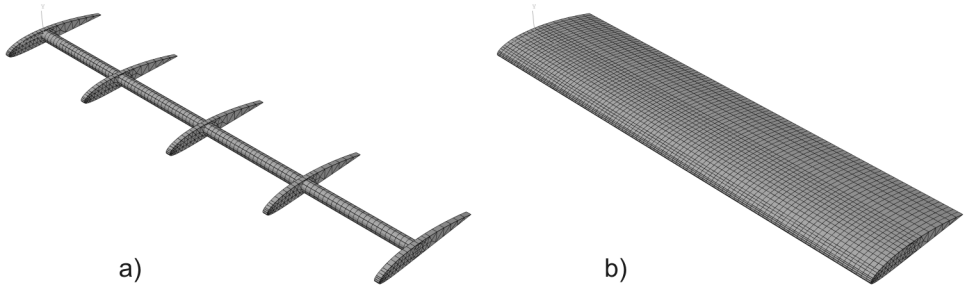

Figure 1. A finite element mesh of an adaptive wing: (a) view without and (b) with the outer skin.

During the analysis presented in the paper an specific activation scenario is used. During this activation process only one actuator is activated and then deactivated. The calculated values of longitudinal strain for the assumed value of the activation moment (0.2 Nm) were equal to 97 μm/m. The numerical simulation shows that the activation process of one SMA actuator results in changes in longitudinal strain on outer skin only at activated section. The received results are similar independent on which SMA actuator was activated. So in the Figure 2 are presented strain profiles (hysteresis) calculated numerically for activation and deactivation processes for one SMA actuator under different value of activation moment.

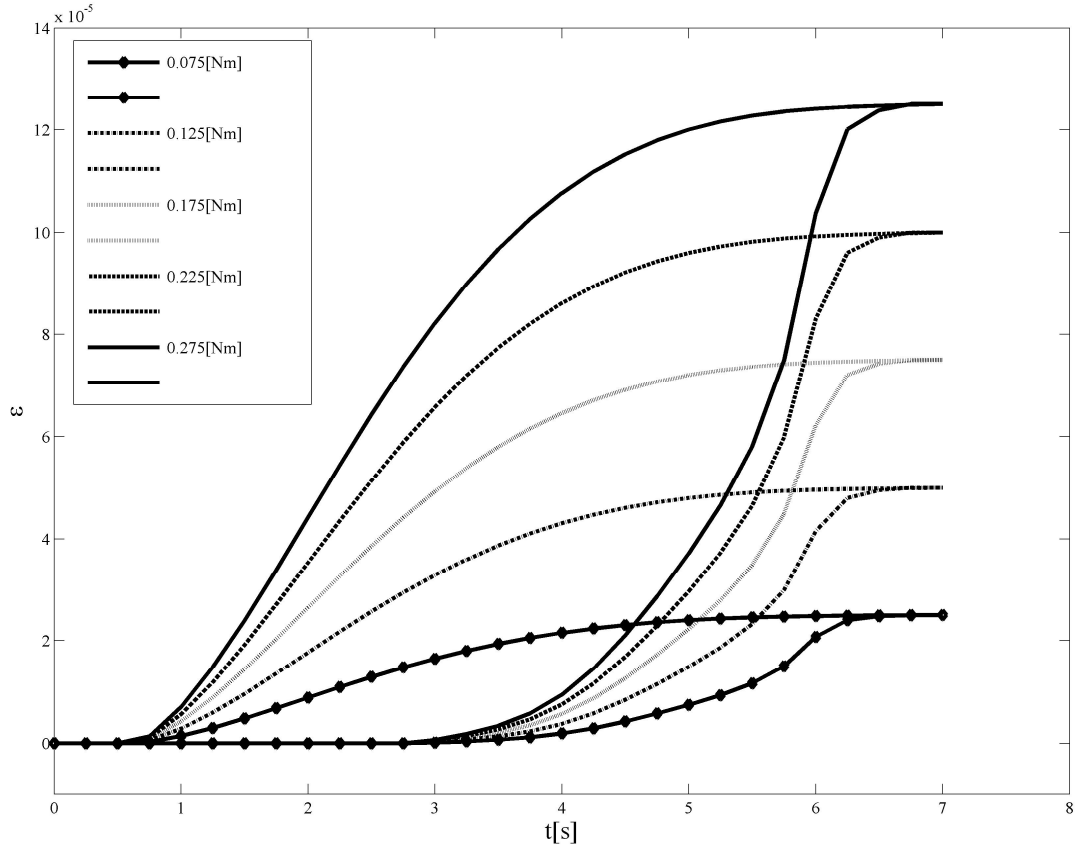

Figure 2. Strain profiles calculated for activation and deactivation processes of one SMA actuator received for different values of the activation moment.

3. Strain measurement using FBG sensors

The longitudinal strain on the outer skin was then measured using FBG sensors configuration presented in the Figure 3. On the outer skin of the wing an array of five FBG sensors was mounted. Four sensors (denoted as S_2–S_5) are FBG strain sensors introduced to measure the longitudinal strain, while the sensor denoted as S_1 is an FBG temperature compensation sensor. Each FBG sensor was 10 mm long, glued to the skin by cyanoacrylate and mounted close to the stiffeners.

The experimental results are presented in Figure 4. All strain profiles measured after activation of actuators A_1 to A_3 have similar shapes. They are also similar to parts of hysteresis regarded to activation process (Figure 2). During the activation process of the actuator A_3, the strongest changes in the longitudinal strain are observed for FBG sensor S_2 located on the neighbour section. This is a result of a strong flexibility of the outer skin of the wing and its wrinkling during the activation process. The activation of the SMA actuator A_4 also strongly influence on longitudinal strain measured by the sensor S_2. In the case, the shape of the strain profile receive during the activation process is also different than the assumed one.

Maximal longitudinal strain values measured after full activation of SMA actuators are in the range from 25μm/m (after activation of the actuator A_3) to 250μm/m (after activation of the actuator A_4). Additionally after activation process of any of the SMA actuators changes of longitudinal strain are observed in measurements from all FBG strain sensors, not only by the FBG sensor located on the investigated section.

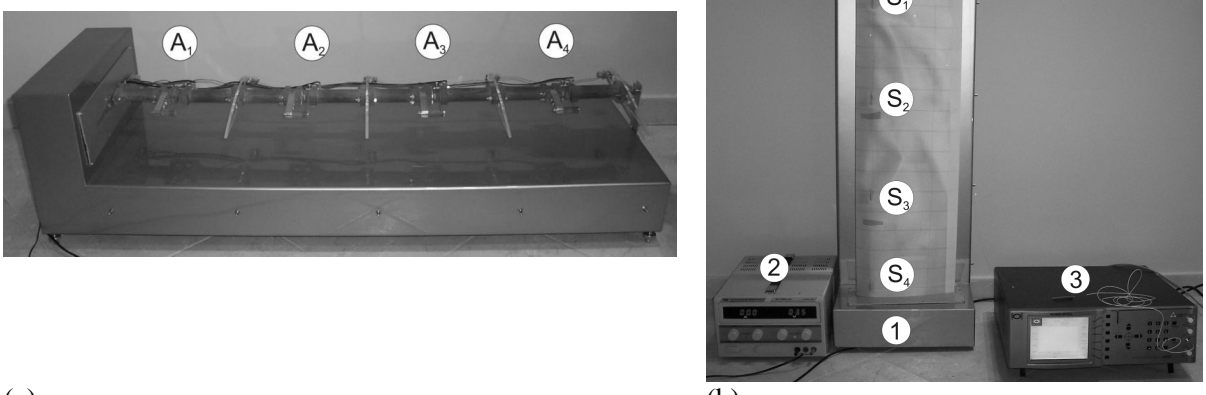

(a) (b)

Figure 3. View of an adaptive wing demonstration stand (a) without outer skin (b) with outer skin and an array of FBG sensors: (1) adaptive wing, (2) controlled DC supply and (3) interrogator.

4. Determination of the real activation moment produced by SMA actuator

The comparison of the results of the measurements presented on the Figure 4 and numerical calculations showed that the real activation moments produced by SMA actuators are different from assumed one, equal to 0.2 Nm. In the purpose of calculation real values of activation moments the results of numerical calculation (Figure 2) and experimental investigation (Figure 4) were compared.

After activation of the actuator A_1 the highest changes in measured longitudinal strain values are observed for the sensor S_5 located on the section. In the case the value of the activation moment is similar to the assumed one and is equal to 0.225Nm.

After activation of the actuator A_2 the highest changes in the strain measured by the FBG sensors are observed for sensor S_4 that is located on the investigated section. However, the maximal value of the longitudinal strain that is observed on the readings from sensor S_3, located on the neighbouring section, is only a half less than for the sensor S_4. Those phenomena are due to location of the SMA actuator and the behaviour of the outer skin of the wing. So, it can be assumed that the real value of the activation moment produced by the SMA actuator A_2 can be calculated based on a sum of longitudinal strains measured by FBG sensors S_3 and S_4. The real value of the activation moment is in this case equal to 0.15Nm.

After the activation of the SMA actuator A_3 the highest change of the longitudinal strain is observed for the sensor S_2 that is installed on the neighbouring section. The maximum value of the longitudinal strain that is measured by the FBG sensor S_3 located on the section is about five times smaller. In this case a similar situation to the previous one is observed. The real value of the activation moment is equal to 0.43Nm.

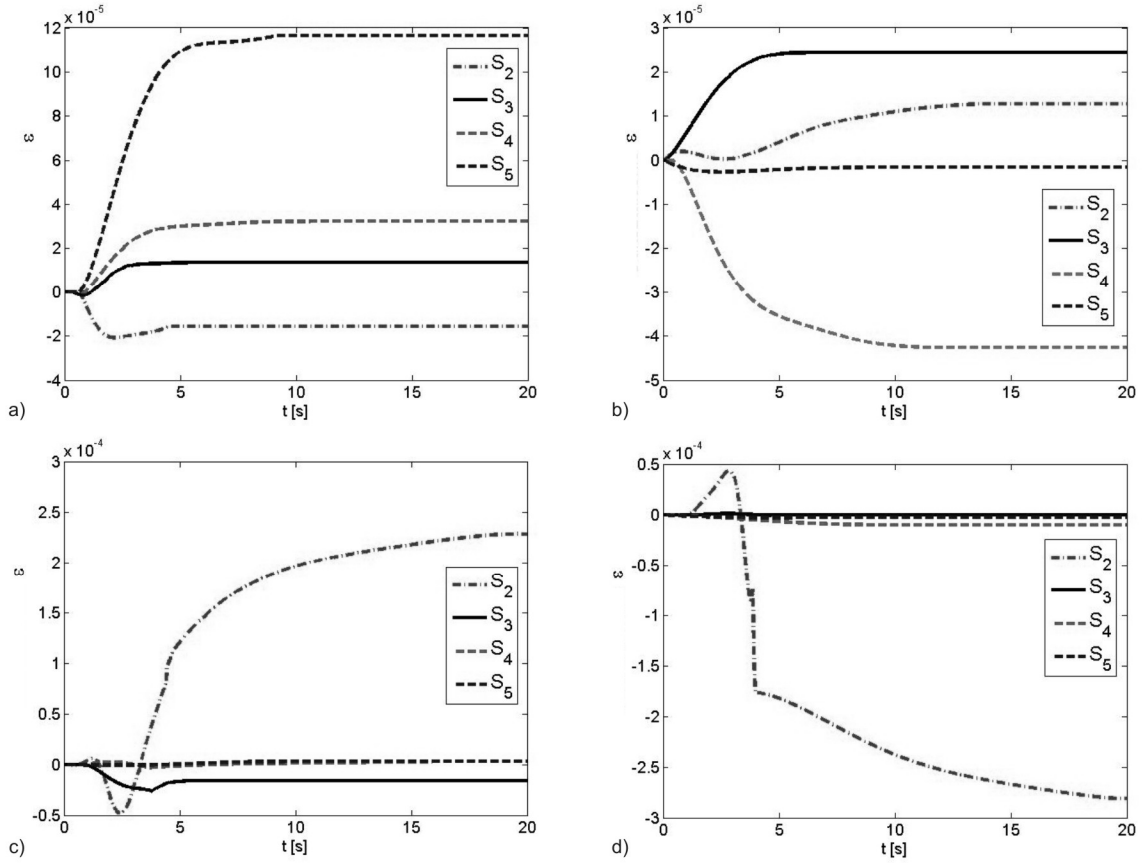

Figure 4. Values of the longitudinal strain measured by FBG sensors ($S_2 – S_5$) after activation of the SMA actuator (a) A_1, (b) A_2, (c) A_3, and (d) A_4.

After activation of the SMA actuator A_4 the highest change of the longitudinal strain is observed for the FBG sensor S_1 that is installed on the investigated section. In this case the real value of the activation moment is equal to 0.54Nm. This value is more that two times larger than it was assumed during the numerical calculation.

After the comparison between the results of the numerical calculations and experimental measurements of the longitudinal strain values it can be claimed that because of the misaligned of the prototype of the adaptive wing the values of the activation moments are different from the assumed one and using during the first numerical calculation. The longitudinal strain calculated for values of the activation moments calculated in the previous paragraph for the same activation scenario are presented on the Figure 5. The value of longitudinal strain received for those activation moments calculating in this paragraph agreed well with values of the longitudinal strain measured by FBG sensors array. The average percentage difference is 4.5%.

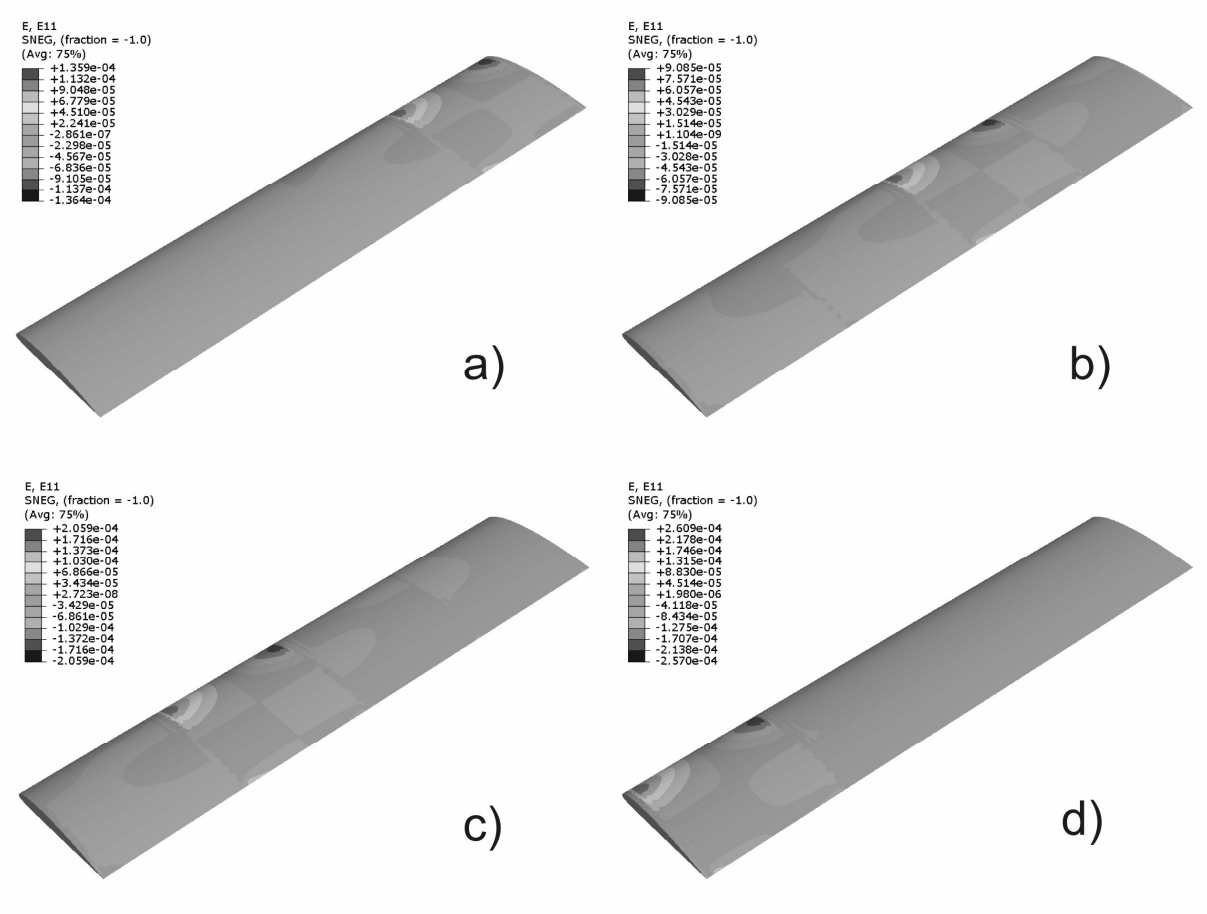

Figure 5. Distribution of the longitudinal strain over the wing surface for second numerical calculation for full activation of SMA actuator (a) A1, (b) A2, (c) A3, and (d) A4.

5. Determination of the level of activation of SMA actuator

One of the problems that can occur for an adaptive wing is the problem with a level of an activation of any of SMA actuators. A continuous monitoring of level of activation as well as determination the end of the deactivation process is very important for safety of the adaptive wing. For this purpose a neural network can be used.

The FBG sensors configuration was used for measurement of strain profiles received during the activation process of SMA actuators. As it was observed during the experiment the values

of longitudinal strain measured by FBG sensors during activation processes of SMA actuators were decreasing. It was a result of decreasing of activation moments. In the Figure 6 and Figure 7 are presented strain hysteresis received for two different SMA actuators after two stages of the activation process.

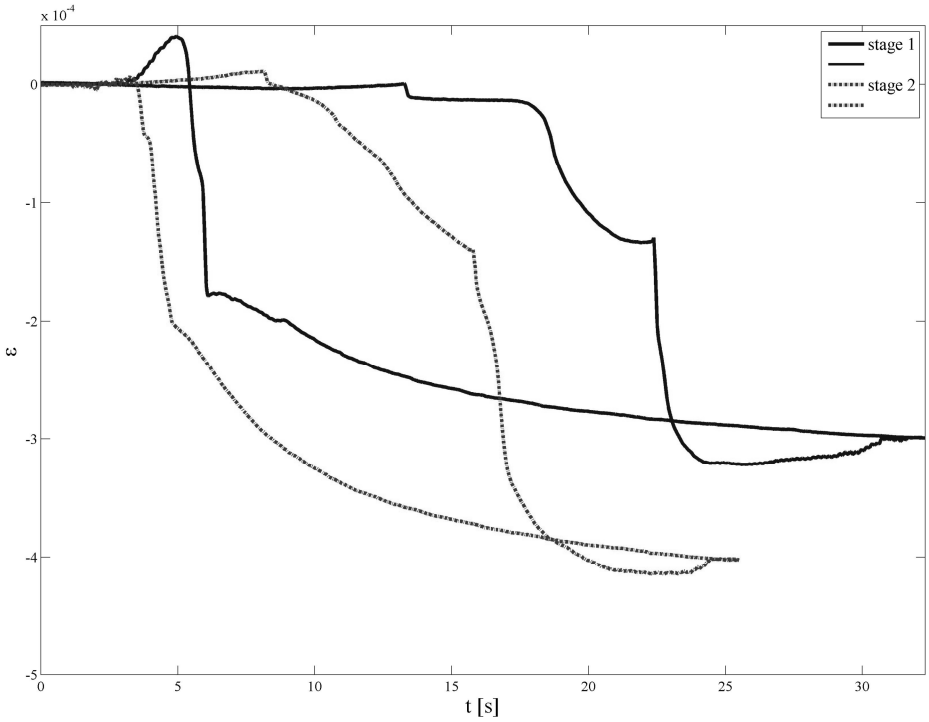

Figure 6. Longitudinal strain measured by FBG sensor S_1 for activation of SMA actuator A_4 for two stages.

Using the FBG sensors configuration mounted on the outer skin of the wing in a combination with neural network a SHM system for an adaptive wing is able to be created. The neural network based on information about the measured strain by FBG sensors is able to determinate the difference between assumed level of activation of particular SMA actuator.

This information allows user to check whether the real shape of the wing after particular activation scenario is agreed well with the prediction. So, it can be determinate which of the SMA actuators is not working properly. The presented system is able to determine the damaged wing section.

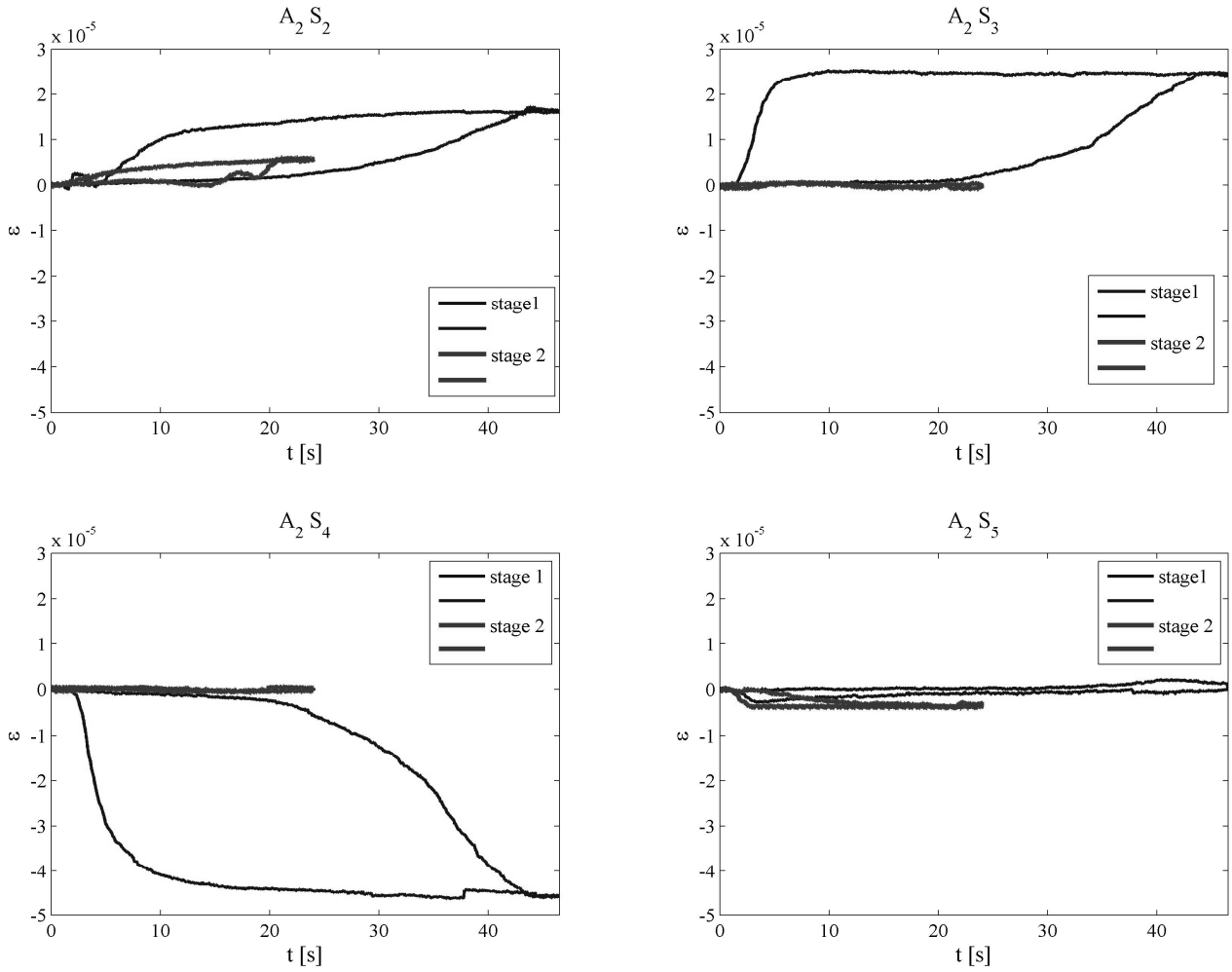

Figure 7. Longitudinal strain measured by FBG sensors for activation of SMA actuator A_2 for two stages.

During the experiment the authors analysed a case when one of the SMA actuators is decreasing its level of activation during consecutive stages of the measurements. On the Figure 8 are presented results of the experiment, while only the SMA actuator A_2 was activated. During the experiment the activation moment of the SMA activation was lowering by loosening the SMA wire being a part of the actuator A_2. For the first stage of the measurement the value of the activation moment was equal to 0.2 Nm, then the value was reduced to 0.15 Nm. Before the beginning of the last stage the activation moment was reduced to almost to 0 Nm.

In the purpose of determining the size of the damage of the actuator the neural networks were applied. In this case the dependence between the longitudinal strains measured by FBG sensors with the value of the activation moment was described. Then the designed neural network was taught to identify the system based on the excitation signal and the real response of the system. Any damage occurrence results in visible changes in parameters of the system and its response. This allows to determine the damage occurrence and monitoring of its

propagation. Increasing of the size of the damage results in larger differences between values of the strain measured at particular moment and its nominal value.

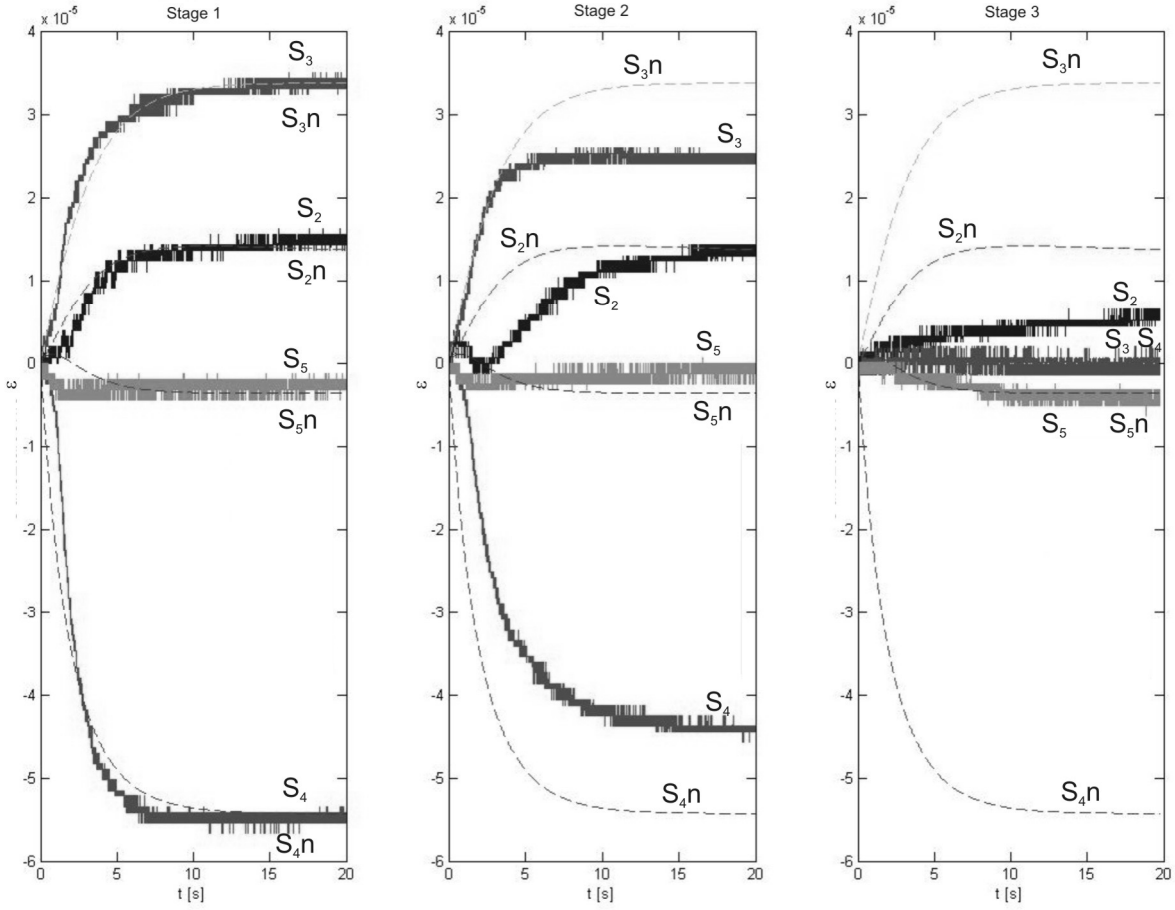

Figure 8. Comparison of longitudinal strain for SMA actuator A_2 measured by FBG sensors (S_2, S_3, S_4, S_5) and calculated using neural networks (S_2n, S_3n, S_4n, S_5n) for three experiments.

During the analysis using neural network only undamaged system was identified. The neural network used in this analysis consisted of two layers. The first of them consisted of 10 neurons with non-linear activation function (hyperbolic tangent) while the second one consisted of 8 neurons with linear activation function. The Levenberg-Marquardt algorithm was used as training method. The number of neurons in output layer depends on the number of evaluated parameters while the number of elements in hidden layer results in accuracy of this evaluation. This allows to determine differences between responses of actual and undamaged systems. Because of fast computing, this method allows operator to watch the differences on the display of monitor or implement proper algorithm of damage assessment.

Conclusions

In the paper an application of neural network for determining the activation moment of the SMA actuators being a part of an adaptive wing is presented and discussed. The activation moments are determining both numerically and experimentally. Real activation moments are different than the assumed ones. The calculated activation moments were then used in

numerical model for determining the values of the longitudinal strain in locations of FBG sensors. The agreement between results achieved for corrected model and experimental measurements using FBG sensors showed good agreement. Additionally the process of degradation of the SMA actuator A_2 is detected using FBG sensors measurements and neural networks.

References

[1] Capolungo P, Ambrosino C, Campopiano S, Cutolo A, Giordano M, Bovio I, Lecce L and Cusano A 2007 Modal analysis and damage detection by fiber Bragg grating sensors Sensors Actuators A 133 415–24
[2] Fuller C R, Elliot S J and Nelson P A 1996 Active Control of Vibration (London: Academic)
[3] Mieloszyk M, Krawczuk M, Zak A, Ostachowicz W 2010 An adaptive wing for a small-aircraft application with a configuration of fibre Bragg grating sensors, Smart Mater. Struct. 19, 085009-085020
[4] Oh J T, Park H C and Hwang W 2001 Active shape control of a double-plate structures using piezoceramics and SMA wires Smart Mater. Struct. 10 1100–6
[5] Ostachowicz W, Krawczuk M and ˙ Zak A 1999 Natural frequencies of a multi-layer composite plate with shape memory alloy wires Int. J. Finite Elem. Anal. 32 71–83
[6] Song G, Kelly B and Agrawal B N 2000 Active position control of a shape memory alloy wire actuated composite beam Smart Mater. Struct. 9 711–6
[7] Takeda S, Aoki Y, Ishikawa T, Takeda N and Kikukawa H 2007 Structural health monitoring of composite wing structure during durability test Compos. Struct. 79 133–9
[8] Zak A, Cartmell M and Ostachowicz W 2003 Dynamics of multilayered composite plates with shape memory alloy wires ASME J. Appl. Mech. 70 313–27
[9] Zak A, Cartmell M and Ostachowicz W 2003 Dynamics and control of a rotor using an integrated SMA/composite active bearing actuator Key Eng. Mater. 245/246 233–40